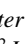


**Yang-Lee edge singularity triggered entanglement transition**Shao-Kai Jian <sup>1,\*</sup>, Zhi-Cheng Yang <sup>2,3,\*</sup>, Zhen Bi <sup>4</sup> and Xiao Chen<sup>5</sup><sup>1</sup>*Condensed Matter Theory Center, Department of Physics, University of Maryland, College Park, Maryland 20742, USA*<sup>2</sup>*Joint Quantum Institute, University of Maryland, College Park, Maryland 20742, USA*<sup>3</sup>*Joint Center for Quantum Information and Computer Science, University of Maryland, College Park, Maryland 20742, USA*<sup>4</sup>*Department of Physics, The Pennsylvania State University, University Park, Pennsylvania 16802, USA*<sup>5</sup>*Department of Physics, Boston College, Chestnut Hill, Massachusetts 02467, USA* (Received 20 January 2021; revised 14 July 2021; accepted 20 September 2021; published 11 October 2021)

We show that a class of  $\mathcal{PT}$  symmetric non-Hermitian Hamiltonians realizing the Yang-Lee edge singularity exhibits an entanglement transition in the long-time steady state evolved under the Hamiltonian. Such a transition is induced by a level crossing triggered by the critical point associated with the Yang-Lee singularity and hence is first order in nature. At the transition, the entanglement entropy of the steady state jumps discontinuously from a volume-law to an area-law scaling. We exemplify this mechanism using a one-dimensional transverse field Ising model with additional imaginary fields, as well as the spin-1 Blume-Capel model and the three-state Potts model. We further make a connection to the forced-measurement induced entanglement transition in a Floquet nonunitary circuit subject to continuous measurements followed by post-selections. Our results demonstrate a new mechanism for entanglement transitions in non-Hermitian systems harboring a critical point.

DOI: [10.1103/PhysRevB.104.L161107](https://doi.org/10.1103/PhysRevB.104.L161107)

*Introduction.* The dynamics of entanglement provides a quantum information perspective on the nonequilibrium dynamics of many-body systems. For chaotic systems—Hamiltonians or random unitary circuits—the entanglement entropy under time evolution typically saturates to a volume-law scaling with the subsystem size, indicating thermalization at late times [1–5]. However, this scenario is altered once the system is coupled to the environment and one tracks an individual quantum trajectory at a time. A minimally structured setup capturing the latter scenario consists of a random unitary circuit interspersed with weak measurements, and a particular sequence of measurement outcome is recorded. Remarkably, such hybrid random unitary circuits feature an entanglement phase transition from a volume-law phase to an area-law phase, as the measurement rate is varied [6–18]. In (1+1) dimensions, this entanglement transition in hybrid random unitary circuits is generically a continuous one exhibiting similar properties vis-à-vis certain nonunitary conformal field theory (CFT) upon mapping to a statistical-mechanics model [7,9,12,19–22].

One expects that the existence of temporal randomness (randomness in gate compositions, measurement locations, and measurement outcomes) is crucial for the universality class of hybrid random unitary circuits, as randomness is typically relevant in lower dimensions [23]. It is thus of great interest to ask whether there can be new possibilities or mechanisms for entanglement transitions in systems where all randomness is removed. One such example is a system subject to continuous weak measurements, and one post-selects a trajectory with a specified outcome. The time evolution in this case can be generated by a non-Hermitian nonrandom

Hamiltonian with an imaginary field, for which one may infer the long-time steady state [24] solely from the eigenvalues and eigenstates. Recent works have identified entanglement transitions in non-Hermitian systems of free fermions [25], chaotic spin chains [26], and the Sachdev-Ye-Kitaev chain in the large  $N$  limit [27]. Nonetheless, the existence and nature of entanglement transitions in non-Hermitian systems remain to be better understood.

In this work, we demonstrate a new mechanism leading to a first-order entanglement transition in a class of  $\mathcal{PT}$  symmetric non-Hermitian Hamiltonians, whose ground state (hereafter referring to the state with the smallest real eigenvalue) undergoes a continuous phase transition belonging to the Yang-Lee universality class [28–32]. The Hamiltonian we consider takes the form

$$H = H_1 + iH_2, \quad (1)$$

where  $H_1$  is a Hermitian interacting Hamiltonian and  $H_2$  denotes an imaginary field. If the ground state of  $H_1$  is in the paramagnetic phase, due to  $\mathcal{PT}$  symmetry, as the imaginary field increases, the ground state and first excited state energies remain real until the gap closes at the Yang-Lee critical point, after which they start splitting in pairs along the imaginary axis. The development of magnetic ordering in the ground state past the critical point continues driving the growth of its imaginary eigenenergy, which eventually leads to a level crossing along the imaginary axis with some (typically) highly excited state. See Fig. 1(a) for an illustration [33]. Since the long-time steady state under time evolution is governed by the right eigenstate with the largest imaginary eigenenergy, this level crossing signals a discontinuous jump in the steady state entanglement from a volume-law to an area-law scaling, because the ground state of  $H_1$  has an area-law scaling entanglement whereas a typical excited state of  $H_1$  has a

\*These authors contributed equally to this work.

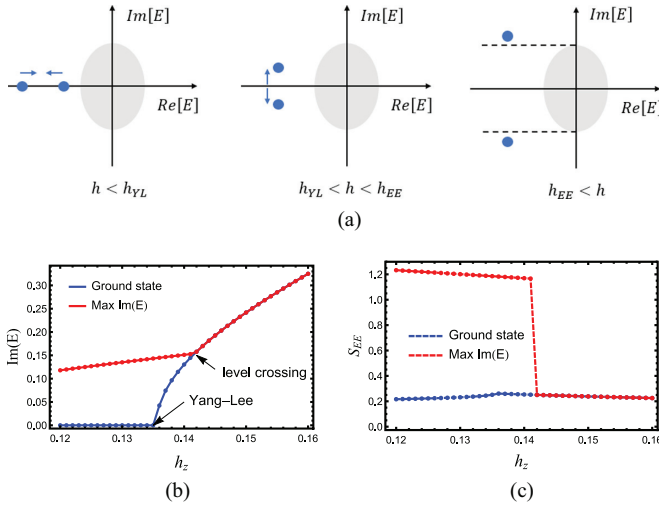


FIG. 1. (a) A schematic of the coalescing-splitting process between the ground state (state with the smallest real eigenvalue) and the first excited state (blue dots). The grey region denotes the (complex) eigenvalues of the rest of the eigenstates. (b), (c) The imaginary part of the eigenenergy (b) and the half-chain entanglement entropy (c) of the ground state (blue) and state with the maximal  $\text{Im}(E)$  (red) as a function of  $h_z$ . We choose  $J = 0.4$ ,  $J_2 = 0.1$ ,  $\Gamma = 1$ ,  $h_y = 0$ , and system size  $L = 10$  with periodic boundary condition.

volume-law scaling entanglement. In contrast, if the ground state of  $H_1$  is in the ordered phase, the steady state is area-law entangled immediately as we introduce  $H_2$ , and hence there is no entanglement transition. We exemplify the above scenario using various one-dimensional quantum spin models with additional imaginary fields, and further make a connection to the forced-measurement induced entanglement transition.

*Yang-Lee edge singularity.* The ferromagnetic phase transition of the classical Ising model in an external magnetic field  $h$  can be understood from the zeros of the partition function on the complex  $h$  plane. Above the critical temperature  $T > T_c$ , all zeros are distributed along the imaginary axis  $|\text{Im}(h)| \geq h_{YL}(T)$ , with  $h_{YL}(T)$  vanishing as  $T$  approaches  $T_c$  [28,29]. The Yang-Lee edge singularity  $h_{YL}$  in fact can be regarded as a conventional critical point described by a  $\phi^3$  field theory with imaginary couplings [30,34] (see Supplemental Material for a brief review [35]). As such, the Yang-Lee singularity can be alternatively realized as a *quantum* phase transition in a (1+1)-dimensional non-Hermitian quantum Hamiltonian [36], where the energy gap between the two states with lowest real eigenenergies closes on the real axis and reopens on the imaginary axis in a universal manner across the transition [see Fig. 1(a)]. By tracking the evolution of the eigenenergy levels on the complex plane across the Yang-Lee critical point, we will show that there must be a first-order entanglement transition induced by a level crossing along the imaginary axis of the eigenenergy spectrum.

Consider a one-dimensional (1D) transverse field Ising model with next-nearest-neighbor couplings and in the presence of imaginary fields

$$H = - \sum_{i=1}^L (J\sigma_i^z \sigma_{i+1}^z + J_2 \sigma_i^z \sigma_{i+2}^z + \Gamma \sigma_i^x + ih_z \sigma_i^z + ih_y \sigma_i^y), \quad (2)$$

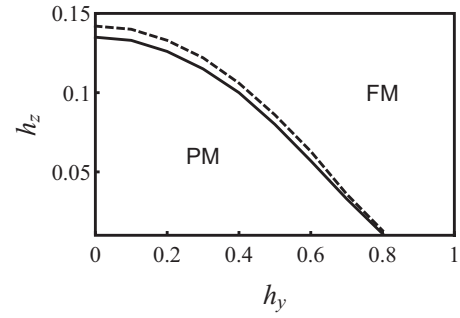


FIG. 2. The phase diagram of Hamiltonian (2) obtained from exact diagonalization of a chain of  $L = 10$  with periodic boundary condition. The solid line denotes the second-order Yang-Lee critical line, and the dashed line is the first-order entanglement transition. We choose  $J = 0.4$ ,  $J_2 = 0.1$ , and  $\Gamma = 1$ .

where  $\sigma^{x,y,z}$  denotes Pauli matrices, and  $J, J_2, \Gamma, h_z, h_y > 0$  are real parameters. We have included a  $J_2$  term such that Hamiltonian (2) is nonintegrable in the absence of imaginary fields; nevertheless, both the Yang-Lee singularity and the entanglement transition persist when  $J_2 = 0$ . This model, despite being non-Hermitian, has a generalized  $\mathcal{PT}$  symmetry which we define below. Therefore, the eigenvalues of Hamiltonian (2) must either be real or come in complex-conjugate pairs. A single eigenenergy cannot leave the real axis without coalescing with a partner and then splitting in pairs. In particular, this is also the case for the ground state of Hamiltonian (2). In spite of the similarity between Hamiltonian (2) and the models studied in Refs. [25,26], we point out that those models do *not* have a Yang-Lee singularity, and hence the mechanisms for the entanglement transition therein are completely different from Hamiltonian (2).

When  $h_y = 0$ , Hamiltonian (2) belongs to the same universality class as the 2D classical Ising model, and the Yang-Lee singularity is realized at  $h_z \neq 0$  in the paramagnetic phase with  $\Gamma > J$  [36]. Since the ground state of Hamiltonian (2) is nondegenerate in the paramagnetic phase, its energy remains real upon increasing  $h_z$  until the gap to the first excited state closes at the critical point, as shown in Fig. 1(a). When the gap reopens past the critical point, the doubly degenerate ground states split in pairs along the imaginary axis and acquire a magnetic order. When  $h_y \neq 0$ , it turns out that Hamiltonian (2) can be brought to the same form as when  $h_y = 0$  via a similarity transformation [37]

$$H' = - \sum_i (J\sigma_i^z \sigma_{i+1}^z + J_2 \sigma_i^z \sigma_{i+2}^z + \tilde{\Gamma} \sigma_i^x + ih_z \sigma_i^z), \quad (3)$$

where  $H$  and  $H'$  are connected by an operator  $\rho$ , i.e.,  $H' = \rho H \rho^{-1}$ , and  $\tilde{\Gamma} = \sqrt{\Gamma^2 - h_y^2}$ , provided that  $|h_y| < |\Gamma|$ . Since Hamiltonian (3) has a  $\mathcal{PT}$  symmetry  $\mathcal{PT} = \prod_{i=1}^L \sigma_i^x \mathcal{K}$ , Hamiltonian (2) also has a generalized  $\mathcal{PT}$  symmetry:  $\mathcal{PT} = \rho \prod_{i=1}^L \sigma_i^x \mathcal{K}$ , where  $\mathcal{K}$  denotes complex conjugation. Thus, a nonzero  $h_y$  simply attenuates the effective strength of the transverse field  $\Gamma$ , and the Yang-Lee singularity persists for a range of nonzero  $h_y$ . The phase diagram of Hamiltonian (2) is shown in Fig. 2. Qualitatively, this phase diagram can be obtained using a mean-field theory of Hamiltonian (2) [35].

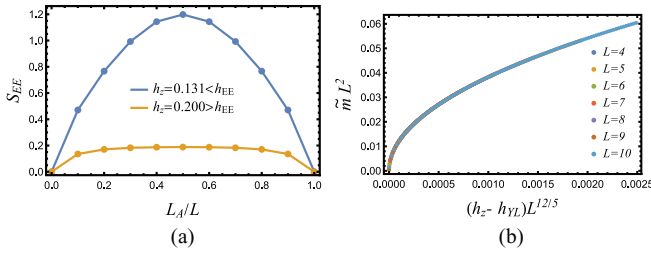


FIG. 3. (a) Scaling of the entanglement entropy as a function of subsystem sizes before and after the level crossing. (b) Data collapse of  $\tilde{m}$  as a function of  $(h_z - h_{YL})$  for different system sizes. The choices of parameters are the same as in Fig. 1.

Since there is only one relevant direction for the Yang-Lee critical point, we shall hereafter fix  $h_y = 0$  and vary  $h_z$ .

*Entanglement transition.* We are interested in the entanglement properties of the long-time steady state evolved under Hamiltonian (2)

$$|\psi(t)\rangle = \frac{e^{-iHt}|\psi_0\rangle}{\|e^{-iHt}|\psi_0\rangle\|}, \quad (4)$$

for  $t \gg 1$ , where  $|\psi_0\rangle$  is an unentangled initial state. In the long-time limit,  $|\psi(t)\rangle$  is dominated by the eigenstate of  $H$  whose imaginary part of the eigenenergy  $\text{Im}(E)$  is the largest. It is thus possible to infer the entanglement property of the long-time steady state from a *single* eigenstate with the largest  $\text{Im}(E)$ . In Fig. 1(b), we plot  $\text{Im}(E)$  for the ground state and the eigenstate with the largest  $\text{Im}(E)$  as  $h_z$  increases. Remarkably, we find a level crossing in  $\text{Im}(E)$  shortly after the Yang-Lee edge singularity, when the ground state takes over to be the one with the largest  $\text{Im}(E)$ . Due to  $\mathcal{PT}$  symmetry, two eigenvalues must coalesce before wandering off the real axis in pairs. One thus expects that, prior to this level crossing, eigenstates that are most likely to develop a large  $\text{Im}(E)$  and hence control the steady state are those located near the middle of the spectrum, where level spacings are the smallest and scale as  $2^{-L}$ . Since these eigenstates are inherited from the excited states of the chaotic Hermitian Hamiltonian  $H_1$ , we expect them to continue exhibiting a volume-law entanglement entropy upon turning on  $H_2$ , as long as the non-Hermitian part is not too large. The volume-law entanglement scaling of such eigenstates in the presence of  $H_2$  is numerically demonstrated in Figs. 3(a) and 4(b) (see below). On the other hand, the ground state is close to a product state with low entanglement obeying an area-law scaling with the subsystem size. Therefore, such a level crossing gives rise to a first-order entanglement transition in the long-time steady state, across which the entanglement jumps discontinuously from a volume-law to an area-law scaling. In Fig. 1(c), we show that the half-chain entanglement entropy of the maximal  $\text{Im}(E)$  eigenstate indeed exhibits a discontinuous jump at the level crossing. The scaling of the entanglement entropy before and after the jump with subsystem sizes shown in Fig. 3(a) also confirms the volume-to-area-law nature of the transition [38].

This first-order entanglement transition, although seemingly coincidental, is in fact *guaranteed* by the Yang-Lee singularity. First of all, the ground state energy can acquire

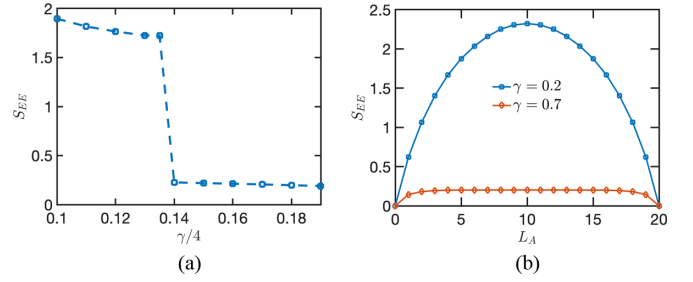


FIG. 4. (a) Entanglement entropy of the steady state under the hybrid circuit evolution (8) as a function of  $\gamma$  for  $L = 16$ . (b) Scaling of the steady state entanglement entropy at measurement rates  $\gamma < \gamma_{EE}$  and  $\gamma > \gamma_{EE}$ , respectively, for  $L = 20$ . We choose  $J = 0.4$ ,  $J_2 = 0.1$ ,  $\Gamma = 1$ ,  $\tau = 0.1$ , and periodic boundary condition.

a nonzero imaginary part solely due to the existence of a critical point where the ground state becomes degenerate, as required by  $\mathcal{PT}$  symmetry. Secondly, the development of ferromagnetic ordering in the ground state past the Yang-Lee singularity guarantees that the ground state will eventually have the largest  $\text{Im}(E)$ . An observation of Hamiltonian (2) yields  $\text{Im}(E) \propto \tilde{m}L$  for an eigenstate, where  $\tilde{m} \equiv \frac{1}{L} \sum_i \langle \sigma_i^z \rangle$  is the average magnetization of this eigenstate [39]. One thus expects that the ferromagnetically ordered ground state has the largest magnetization and hence its  $\text{Im}(E)$  must dominate over states near the middle of the spectrum in the thermodynamic limit. Therefore, although the long-time steady state by itself is blind to the critical point, the very existence of which in fact triggers a subsequent level crossing, when the steady state switches character from a highly entangled state in the middle of the spectrum to an ordered ground state with low entanglement.

To further show that the first-order entanglement transition happens at a finite distance past the critical point in the thermodynamic limit, we employ a finite-size scaling analysis of the onset of  $\text{Im}(E)$  in the vicinity of the critical point. Since the Yang-Lee critical point has a dynamical critical exponent  $z = 1$ , it is natural to expect that the (imaginary) energy density  $\tilde{m} \propto \text{Im}(E)/L$  should satisfy the following scaling form:

$$\tilde{m} = L^{-2} f_{\tilde{m}}\left((h_z - h_{YL})L^{\frac{d+2-\eta}{2}}\right), \quad h_z > h_{YL}, \quad (5)$$

where  $f_{\tilde{m}}$  is a universal scaling function with  $f_{\tilde{m}}(0) = 0$ , and  $\eta$  is the anomalous dimension. In order to have a sensible scaling form in the thermodynamic limit, the scaling function must satisfy  $f_{\tilde{m}}(x) \sim x^{\frac{4}{d+2-\eta}}$  as  $x \rightarrow \infty$ , yielding  $\tilde{m} \sim (h_z - h_{YL})^{\frac{4}{d+2-\eta}}$  in the thermodynamic limit. For the (1+1)D Yang-Lee singularity that we focus on here,  $d = 2$ , and the corresponding nonunitary CFT data give  $\eta = -4/5$  [31,35]. The scaling form thus becomes  $\tilde{m}L^2 = f_{\tilde{m}}((h_z - h_{YL})L^{12/5})$ . This relation is demonstrated perfectly in Fig. 3(b). We thus obtain the following universal scaling form of  $\tilde{m}$  of the ground state near the Yang-Lee singularity in the thermodynamic limit (with  $\lambda > 0$ ):

$$\tilde{m} \approx \lambda (h_z - h_{YL})^{5/6}, \quad h_z > h_{YL}. \quad (6)$$

Equation (6) implies that  $\tilde{m}$  continuously increases from zero in the thermodynamic limit, and hence the first-order entanglement transition must happen at a finite distance past the

critical point when  $\tilde{m}$  of the ground state supersedes that of the previously dominating eigenstate. If one instead starts from the ferromagnetic phase of Hamiltonian (2), this entanglement transition is absent. Since the ground state is twofold degenerate to begin with, an infinitesimal  $h_z$  will immediately drive the steady state to an area-law phase.

We remark that the mechanism underlying the entanglement transition as being triggered by a critical point is different from that in recently studied non-Hermitian systems where a critical point is absent [26]. In the Supplemental Material, we show that the ground state of the model studied therein remains nondegenerate with real energy at all times, due to the absence of a quantum phase transition [35]. Therefore, a level crossing is not guaranteed, and the entanglement entropy of the steady state evolves continuously once the spectrum becomes complex.

*Forced-measurement induced entanglement transition.* It is useful to connect the time evolution under the non-Hermitian Hamiltonian (2) to a system undergoing repeated weak measurements and post-selections. Consider the following circuit. In each time step of duration  $\tau$ , the circuit consists of a unitary time evolution  $U = e^{-iH_0\tau}$  with  $H_0 = -\sum_{i=1}^L (J\sigma_i^z\sigma_{i+1}^z + J_2\sigma_i^z\sigma_{i+2}^z + \Gamma\sigma_i^x)$ , followed by weak measurements corresponding to the following set of Kraus operators:

$$M_0^{(i)} = 1 - (1 - \sqrt{1 - \gamma\tau})\Pi_i, \quad M_z^{(i)} = \sqrt{\gamma\tau}\Pi_i, \quad (7)$$

where  $\Pi_i = \frac{1}{2}(\sigma_i^z + 1)$  is a projector to the spin-up state at site  $i$ . If the post-selection is conditioned on  $M_0^{(i)}$ , the time evolution with  $M_0 = \otimes_{i=1}^L M_0^{(i)}$ ,

$$|\psi(N\tau)\rangle = \frac{(M_0U)^N |\psi_0\rangle}{\|(M_0U)^N |\psi_0\rangle\|}, \quad (8)$$

in the limit  $\gamma\tau \ll 1$ , is then precisely generated by the non-Hermitian Hamiltonian (2) with  $h_z = \gamma/4$  and  $h_y = 0$ . In general, one can rotate the spin polarization direction in the  $y$ - $z$  plane along which measurements are performed so as to realize Hamiltonian (2) with arbitrary  $h_y$  and  $h_z$ . The entanglement transition in this context is also known as a forced-measurement-induced phase transition [40]. Namely, when the measurement rate is finite but smaller than a threshold  $\gamma < \gamma_{EE}$ , the hybrid circuit is able to evolve an unentangled initial state to a final state with volume-law entanglement; whereas when the measurement rate is large  $\gamma > \gamma_{EE}$ , the time-evolved state remains area-law entangled. We simulate the time evolution (8) for system size up to  $L = 20$  using Krylov space time evolution method [41], and compute the entanglement entropy for different measurement rates, as shown in Fig. 4. We indeed find a similar entanglement transition in the steady state from a volume-law to an area-law scaling, as the measurement rate increases [35]. Such a forced-measurement-induced entanglement transition can now be elegantly accounted for by a Yang-Lee edge singularity triggered level crossing in the eigenspectrum of the corresponding non-Hermitian Hamiltonian [35]. Since this transition is first order, it is distinct from the continuous transitions driven by weak measurements where there is intrinsic randomness in the outcomes [7].

*Spin-1 Blume-Capel model.* To demonstrate that this mechanism for entanglement transition extends beyond the simple

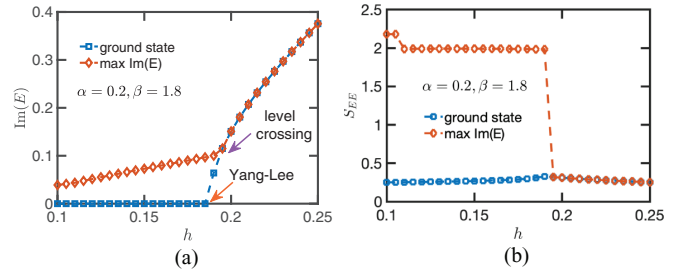


FIG. 5. (a) Imaginary part of the eigenvalues for the ground state and eigenstate with the largest  $\text{Im}(E)$  of Hamiltonian (9). (b) Entanglement entropy of the same sets of states as in (a). We choose  $\alpha = 0.2$ ,  $\beta = 1.8$ , and system size  $L = 6$  with periodic boundary condition.

Hamiltonian (2), we now show another quantum spin chain realization of the Yang-Lee edge singularity, where the critical point also triggers a subsequent entanglement transition. Consider the quantum spin-1 Blume-Capel model described by the Hamiltonian

$$H = \sum_i [\alpha(S_i^z)^2 + \beta S_i^x - S_i^z S_{i+1}^z - ihS_i^z], \quad (9)$$

where  $S_i^{x,y,z}$  are  $3 \times 3$  spin-1 matrices. This model has a rich phase diagram, as shown in Ref. [42]. In the absence of an imaginary field  $h = 0$ , Hamiltonian (9) has an ordered phase with broken  $\mathbb{Z}_2$  symmetry and a disordered phase separated by a single critical curve starting at  $\alpha = 1$  and  $\beta = 0$ , and moving towards smaller values of  $\alpha$  upon increasing  $\beta$ . In the disordered phase, further turning on the imaginary field  $h$  drives a continuous transition with  $c = -22/5$  corresponding to the Yang-Lee universality class.

In Fig. 5(a), we plot the imaginary part of the eigenvalues for the ground state and eigenstate with the largest  $\text{Im}(E)$  of Hamiltonian (9) as a function of  $h$ . Similar to Hamiltonian (2), here we also find a level crossing slightly past the Yang-Lee singularity, after which the ground state becomes the one with the largest  $\text{Im}(E)$ . We thus expect that the steady state entanglement entropy will also exhibit a discontinuous jump from a volume-law scaling to an area-law scaling, as is confirmed numerically in Fig. 5(b). Since the ground state develops a large magnetization  $\langle S^z \rangle$  after transitioning to the ordered phase, we argue that the imaginary part of the ground state energy, which is proportional to  $\langle S^z \rangle L$ , must dominate over all other eigenstates. Therefore, this level crossing, and hence the first-order entanglement transition, persists in the thermodynamic limit.

So far, we have been focusing on non-Hermitian Hamiltonians with  $\mathcal{PT}$  symmetry as a cleanest exemplification of our general idea. However, we remark that  $\mathcal{PT}$  symmetry is *not* a necessary condition for the entanglement transition to happen, as long as the system harbors a critical point. In the Supplemental Material, we give an example of the quantum three-state Potts model with an imaginary field, which does not have  $\mathcal{PT}$  symmetry but nevertheless possesses the Yang-Lee edge singularity [35]. We find that the same story holds in this case as well.

*Concluding remarks.* In this work, we demonstrate a new mechanism where a class of non-Hermitian Hamiltonians



realizing the Yang-Lee edge singularity further triggers a first-order entanglement transition in the long-time steady state. This entanglement phase transition can also be understood in terms of the purification dynamics [10,11,35]. Notice that the purification rate is determined by the gap between the largest and second largest  $\text{Im}(E)$ . In the area-law phase, the entropy of an initially mixed density matrix decays at a finite constant rate and the purification time scales as  $\log L$ . In contrast, in the volume-law phase, the purification time is much longer, presumably exponential in the system size. The mechanism for entanglement transitions uncovered in this work also provides new insight on nonunitary dynamics from the perspective of quantum trajectories. If post-selections are removed or some randomness is introduced in our model, we expect that this first-order transition will be rounded to a continuous one [43,44]. We leave a detailed study on this for future work.

*Acknowledgments.* We thank Michael Gullans for useful comments on the manuscript, and Sarang Gopalakrishnan and Thomas Iadecola for helpful discussions. S.-K.J. is supported by the Simons Foundation via the It From Qubit Collaboration. Z.-C.Y. acknowledges funding by the DOE ASCR Accelerated Research in Quantum Computing program (Award No. DE-SC0020312), U.S. Department of Energy Award No. DE-SC0019449, the DOE ASCR Quantum Testbed Pathfinder program (Award No. DE-SC0019040), the NSF PFCQC program, AFOSR, ARO MURI, AFOSR MURI, and NSF PFC at JQI. Z.-C.Y. is also supported by MURI ONR N00014-20-1-2325, MURI AFOSR, FA9550-19-1-0399, and the Simons Foundation. Part of the numerical calculations were performed on the Boston University Shared Computing Cluster, which is administered by Boston University Research Computing Services.

- 
- [1] H. Kim and D. A. Huse, *Phys. Rev. Lett.* **111**, 127205 (2013).
- [2] L. Zhang, H. Kim, and D. A. Huse, *Phys. Rev. E* **91**, 062128 (2015).
- [3] W. W. Ho and D. A. Abanin, *Phys. Rev. B* **95**, 094302 (2017).
- [4] A. Nahum, J. Ruhman, S. Vijay, and J. Haah, *Phys. Rev. X* **7**, 031016 (2017).
- [5] T. Zhou and A. Nahum, *Phys. Rev. B* **99**, 174205 (2019).
- [6] Y. Li, X. Chen, and M. P. A. Fisher, *Phys. Rev. B* **98**, 205136 (2018).
- [7] Y. Li, X. Chen, and M. P. A. Fisher, *Phys. Rev. B* **100**, 134306 (2019).
- [8] A. Chan, R. M. Nandkishore, M. Pretko, and G. Smith, *Phys. Rev. B* **99**, 224307 (2019).
- [9] B. Skinner, J. Ruhman, and A. Nahum, *Phys. Rev. X* **9**, 031009 (2019).
- [10] M. J. Gullans and D. A. Huse, *Phys. Rev. X* **10**, 041020 (2020).
- [11] M. J. Gullans and D. A. Huse, *Phys. Rev. Lett.* **125**, 070606 (2020).
- [12] R. Fan, S. Vijay, A. Vishwanath, and Y.-Z. You, *Phys. Rev. B* **103**, 174309 (2021).
- [13] S. Choi, Y. Bao, X.-L. Qi, and E. Altman, *Phys. Rev. Lett.* **125**, 030505 (2020).
- [14] J. Iaconis, A. Lucas, and X. Chen, *Phys. Rev. B* **102**, 224311 (2020).
- [15] S. Sang and T. H. Hsieh, *Phys. Rev. Research* **3**, 023200 (2021).
- [16] A. Lavasani, Y. Alavirad, and M. Barkeshli, *Nat. Phys.* **17**, 342 (2021).
- [17] A. Lavasani, Y. Alavirad, and M. Barkeshli, [arXiv:2011.06595v](https://arxiv.org/abs/2011.06595v).
- [18] M. Ippoliti, M. J. Gullans, S. Gopalakrishnan, D. A. Huse, and V. Khemani, *Phys. Rev. X* **11**, 011030 (2021).
- [19] R. Vasseur, A. C. Potter, Y.-Z. You, and A. W. W. Ludwig, *Phys. Rev. B* **100**, 134203 (2019).
- [20] C.-M. Jian, Y.-Z. You, R. Vasseur, and A. W. W. Ludwig, *Phys. Rev. B* **101**, 104302 (2020).
- [21] Y. Li, X. Chen, A. W. Ludwig, and M. Fisher, *Phys. Rev. B* **104**, 104305 (2021).
- [22] Y. Bao, S. Choi, and E. Altman, *Phys. Rev. B* **101**, 104301 (2020).
- [23] A. B. Harris, *J. Phys. C* **7**, 1671 (1974).
- [24] Notice that the states here are not really steady, since the wave function is not normalized due to the nonunitary evolution. Nonetheless, here we use the name to refer to eigenstate with the largest imaginary eigenvalue, so that it dominates the wave function in the long-time limit.
- [25] A. Biella and M. Schiró, *Quantum* **5**, 528 (2021).
- [26] S. Gopalakrishnan and M. J. Gullans, *Phys. Rev. Lett.* **126**, 170503 (2021).
- [27] C. Liu, P. Zhang, and X. Chen, *SciPost Phys.* **10**, 048 (2021).
- [28] C. N. Yang and T. D. Lee, *Phys. Rev.* **87**, 404 (1952).
- [29] T. D. Lee and C. N. Yang, *Phys. Rev.* **87**, 410 (1952).
- [30] M. E. Fisher, *Phys. Rev. Lett.* **40**, 1610 (1978).
- [31] J. L. Cardy, *Phys. Rev. Lett.* **54**, 1354 (1985).
- [32] N. Matsumoto, M. Nakagawa, and M. Ueda, [arXiv:2012.13144](https://arxiv.org/abs/2012.13144).
- [33] See [35] for a concrete realization of Fig. 1(a) in Eq. (2).
- [34] P. J. Kortman and R. B. Griffiths, *Phys. Rev. Lett.* **27**, 1439 (1971).
- [35] See Supplemental Material at <http://link.aps.org/supplemental/10.1103/PhysRevB.104.L161107> for a review of the Yang-Lee edge singularity, mean-field theory of Hamiltonian (2), scaling analysis of the Yang-Lee singularity in Hamiltonian (2), purification rate of Hamiltonian (2), additional numerical results on the circuit model, entanglement transition in a quantum three-state Potts model, and a non-Hermitian Hamiltonian studied in Ref. [26] without Yang-Lee edge singularity, which includes Refs. [45,46].
- [36] G. Von Gehlen, *J. Phys. A: Math. Gen.* **24**, 5371 (1991).
- [37] T. Deguchi and P. K. Ghosh, *J. Phys. A: Math. Theor.* **42**, 475208 (2009).
- [38] Due to a finite non-Hermitian part, the volume law coefficient is much less than the thermal value at  $h_z = 0$ .
- [39] Notice that the magnetization referred to here as being a  $\sigma^z$  sandwiched between two right eigenvectors is *not* the order parameter associated with the corresponding field theory, which is a  $\sigma^z$  sandwiched between a left and a right eigenvector and satisfies the scaling relation  $m \sim (h - h_c)^{1/\delta}$ . We draw a distinction by adding a tilde to the quantity we defined here:  $\tilde{m}$ .

- [40] A. Nahum, S. Roy, B. Skinner, and J. Ruhman, [PRX Quantum](#) **2**, 010352 (2021).
- [41] D. J. Luitz and Y. B. Lev, [Ann. Phys. \(NY\)](#) **529**, 1600350 (2017).
- [42] G. V. Gehlen, in *Perspectives On Solvable Models* (World Scientific, Singapore, 1994), pp. 59–81.
- [43] M. Aizenman and J. Wehr, [Phys. Rev. Lett.](#) **62**, 2503 (1989).
- [44] J. Cardy and J. L. Jacobsen, [Phys. Rev. Lett.](#) **79**, 4063 (1997).
- [45] D. Poland, S. Rychkov, and A. Vichi, [Rev. Mod. Phys.](#) **91**, 015002 (2019).
- [46] T. Wydro and J. F. McCabe, [Int. J. Mod. Phys. B](#) **19**, 3021 (2005).